energies

Article

A Hierarchical Met-Ocean Data Selection Model for Fast O&M Simulation in Offshore Renewable Energy Systems

Hailun Xie [1] and Lars Johanning [1,2,*]

[1] Renewable Energy Group, Faculty of Environment, Science, and Economy, University of Exeter, Penryn Campus, Penryn TR10 9FE, UK
[2] College of Shipbuilding Engineering, Harbin Engineering University, Harbin 150001, China
* Correspondence: l.johanning@exeter.ac.uk

Abstract: In this research, a hierarchical met-ocean data selection model is proposed to reduce the computational cost in stochastic simulation of operation and maintenance (O&M) and enable rapid evaluation of offshore renewable energy systems. The proposed model identifies the most representative data for each calendar month from the long-term historical met-ocean data in two steps, namely the preselection and the refined selection. The preselection incorporates three distinct metrics to evaluate the characteristics of statistical distributions, including the Jensen–Shannon divergence, the encapsulation of extreme met-ocean conditions, as well as the overall vessel accessibility. For the refined selection, a component of temporal synchrony is devised to emulate dynamic changes of met-ocean conditions. As such, a met-ocean reference year comprising twelve representative historical months is subsequently produced and deployed as the input for O&M stochastic simulation. While this research focuses on the development of a generalised methodology for selecting representative met-ocean data, the proposed statistical method is validated empirically using a case study inspired by real-life floating offshore wind installations in Scotland, e.g., Hywind and Kincardine projects. According to the O&M simulation results with five capacity scenarios, the proposed data selection model reduces the computational cost by up to 97.65% while emulating the original results with minor deviations, i.e., within ±5%. The simulation speed is therefore 43 times quicker. Overall, the proposed met-ocean data selection model attains an excellent trade off between computational efficiency and accuracy in O&M stochastic simulation.

Keywords: offshore renewable energy; representative year; met-ocean data; O&M; M

check for updates

Citation: Xie, H.; Johanning, L. A Hierarchical Met-Ocean Data Selection Model for Fast O&M Simulation in Offshore Renewable Energy Systems. *Energies* **2023**, *16*, 1471. https://doi.org/10.3390/en16031471

Academic Editors: Eugen Rusu and Madjid Karimirad

Received: 16 November 2022
Revised: 24 January 2023
Accepted: 31 January 2023
Published: 2 February 2023

1. Introduction

Since offshore renewable energy (ORE) plays a pivotal role in decarbonising the global energy sector and tackling climate change, many studies are dedicated to techno-economic analysis of ORE systems, such as offshore wind farms [1,2], wave energy converters [3,4], tidal energy farms [5,6], as well as offshore hydrogen productions [7–9]. One of the key components in techno-economic analysis is the estimation of operation and maintenance (O&M) costs as they have prominent contributions to the lifecycle costs of ORE projects, e.g., 25–30% for offshore wind farms [10]. More specifically, O&M denotes a set of procedures required to keep a system operational for a desired timespan, following its commissioning and installation [11]. The aim of O&M in ORE systems is to ensure reliability and availability of electricity generation with minimum resource allocations and economic costs [12]. O&M strategies can be classified into three major categories according to the level of criticality of components in systems, i.e., corrective maintenance for assets with low criticality, periodic maintenance for assets with a well-known and consistent failure–time correlation, and condition-based maintenance for the most critical assets [12,13]. O&M activities in ORE systems are essentially logistical problems and they become more complicated owing to the increase in distances from ORE sites to the shore and the uncertainties resulted from harsh offshore environments. Various aspects need to be considered in the O&M phase, including the reliability of components in ORE systems, accessibility via vessels, the transfer of components and technicians for repair and replacement, as well as meteorological and oceanographical conditions [14]. Therefore, O&M should be investigated properly in order to determine the optimal maintenance strategies and achieve the trade off between minimizing the cost and maximizing the availability of ORE systems [15].

The estimation of O&M costs is complex due to the interactions among component reliability, vessel accessibility, as well as system availability. To quantify uncertainties and enable probabilistic O&M simulation, O&M assessment tools are often deployed using Markov Chains Monte Carlo (MCMC) techniques [16–20]. These tools are able to imitate the stochastic nature of failure occurrence and mimic realistic constraints in terms of dynamic met-ocean environment, resource availability and vessel limitations. They require decades of met-ocean data, which provide measured combined wind, wave and climate conditions, such as wind speed and direction, wave height and sea condition, temperature and humidity, as the input to determine weather windows and vessel accessibility through the lifetime of ORE projects [21]. Despite their effectiveness, the MCMC-based O&M simulations are characterised by significant computational cost due to the need for multiple simulations to define the distribution of stochastic outputs, such as O&M cost, and the consideration of probabilistic failure occurrence at each timestep in each simulation. Typically, 1000 or 10,000 experimental runs are required for a lifecycle assessment using Monte Carlo simulations [22], and the probabilistic occurrences of component failures need to be simulated on a sub-daily or even hourly basis over the lifespan of ORE systems, i.e., usually 20 to 25 years [23]. The high computational cost becomes a bottleneck in a lifecycle assessment of ORE systems, especially when it comes to the integration of stochastic simulation tools with holistic optimisation since optimisation also incurs significant computational cost [24–26]. As a result, there is an intrinsic trade off between the accuracy and the computational efficiency of O&M stochastic simulations. Similar limitations also exist in energy system design and the ideas of constructing representative hours, days and weeks by aggregating long-term time series data were proposed to reduce computational cost in existing studies [27–29]. The aggregation can be performed in two fashions, namely averaging and time slices. The averaging method aggregates consecutive periods into one period, such as representing one year by twelve monthly averaged representative days [30–32]. The time slice method groups periods based on timeframes, such as seasons, weekends and weekdays [33–36]. Despite the applications in energy system planning and expansion, the existing aggregation methods are not suitable for O&M stochastic simulation since they undermine the sequence and variability of the original time series data, which are critical to the calculation of weather windows in O&M assessment. Therefore, new methods of constructing a representative period need to be developed to reduce the computational cost in O&M stochastic simulation.

In order to overcome the limitation of computational inefficiency and enhance the practicality of O&M stochastic simulation, in this study, a hierarchical statistical model is proposed to identify the most representative historical month from the long-term met-ocean data for each calendar month and generate a met-ocean reference year with one-year equivalent length for an O&M stochastic simulation. Using the yielded met-ocean reference year, the computational efficiency of O&M stochastic simulation can be boosted significantly owing to the major reduction in the input met-ocean time series and the total number of iterations in a Monte Carlo simulation. The proposed model includes two steps: (1) the preselection to produce five candidate historical months and (2) the refined selection to identify the most suitable month from the preselected candidates. The selection process is conducted independently for each calendar month from January to December. In the preselection, three statistical components are incorporated to characterise the similarities between the historical months and the long-term met-ocean data belonging to the same calendar month, including the Jensen–Shannon (JS) divergence [37], the coverage of extreme met-ocean conditions, as well as the availability of met-ocean windows regarding vessel accessibility. In the refined selection, the change patterns of met-ocean conditions between the candidate months and the long-term data from the same calendar month are compared using cosine similarity. As such, the proposed hierarchical model is capable of evaluating similarities on different dimensions, including statistical distribution, temporal synchrony, as well as extreme conditions. The trade off between computational cost and accuracy can be achieved in an O&M stochastic simulation by the proposed data selection model owing to the preserving characteristics of a met-ocean time series in a reduced length.

Inspired by real-life installations of floating offshore wind in Scotland, i.e., Hywind and Kincardine projects, a case study which is representative of the above two projects is developed to evaluate the proposed data selection model, following the existing study [2]. An offshore location halfway between Hywind and Kincardine projects is selected to retrieve met-ocean data owing to the short distance between the two sites, i.e., 47 km. A port located 25 km West of Hywind project, namely Peterhead quay, is considered the O&M base since it satisfies conditions of facilities and infrastructure for installation and operation of floating offshore wind devices [2]. Five capacity scenarios are employed to evaluate the proposed model on different farm sizes in the case study, including 2, 5, 10, 20 and 30 turbines.

The research contributions of this study are highlighted as follows.

1. A hierarchical met-ocean data selection model is proposed to produce a refined representation of met-ocean conditions from the long-term historical record. The generated representative met-ocean data preserves the characteristics of the original long-term met-ocean time series.
2. The representative met-ocean data set generated by the proposed model is employed to reduce the computational cost and enhance the practicality of an O&M stochastic simulation for ORE systems. Based on the empirical results, the computation time can be reduced by up to 97.65% and the simulation speed becomes 43 times faster. Meanwhile, the original simulation results can be reproduced with minor deviations, i.e., within $\pm$ 5%.
3. The distributions of the synthetic lifetime O&M cost and the lifetime energy production are established for the representative met-ocean data set using random sampling. Evidenced by the Wilcoxon rank sum test results, no significant statistical difference is observed on the distributions of the O&M cost between the representative data and the original long-term data, whereas the deviations on the distributions of the lifetime energy production are narrow.

The remainder of the paper is organised as follows: In Section 2, the details of the proposed hierarchical met-ocean data selection model are presented. Section 3 assesses the impact of each statistical component on the selection of met-ocean data. Furthermore, the simulation results of the lifetime O&M cost, the lifetime energy production, as well as the computational time are compared between the single-year representative met-ocean data set and the original long-term met-ocean data set in Section 4. In Section 5, the importance of temporal synchrony for the generation of a representative met-ocean data set and its impact on the O&M simulation are discussed. Finally, the conclusions are drawn and future research directions are presented in Section 6.

2. Methodology

In this research, a hierarchical met-ocean data selection model is proposed to reduce computational cost while retaining simulation accuracy for an O&M stochastic simulation of ORE systems. The overall schematic of the proposed method is shown in Figure 1. The proposed method comprises two stages, i.e., the preselection and the refined selection. For each calendar month, the preselection produces five candidates from all corresponding historical months, whereas the refined selection identifies the most representative month from the candidates.

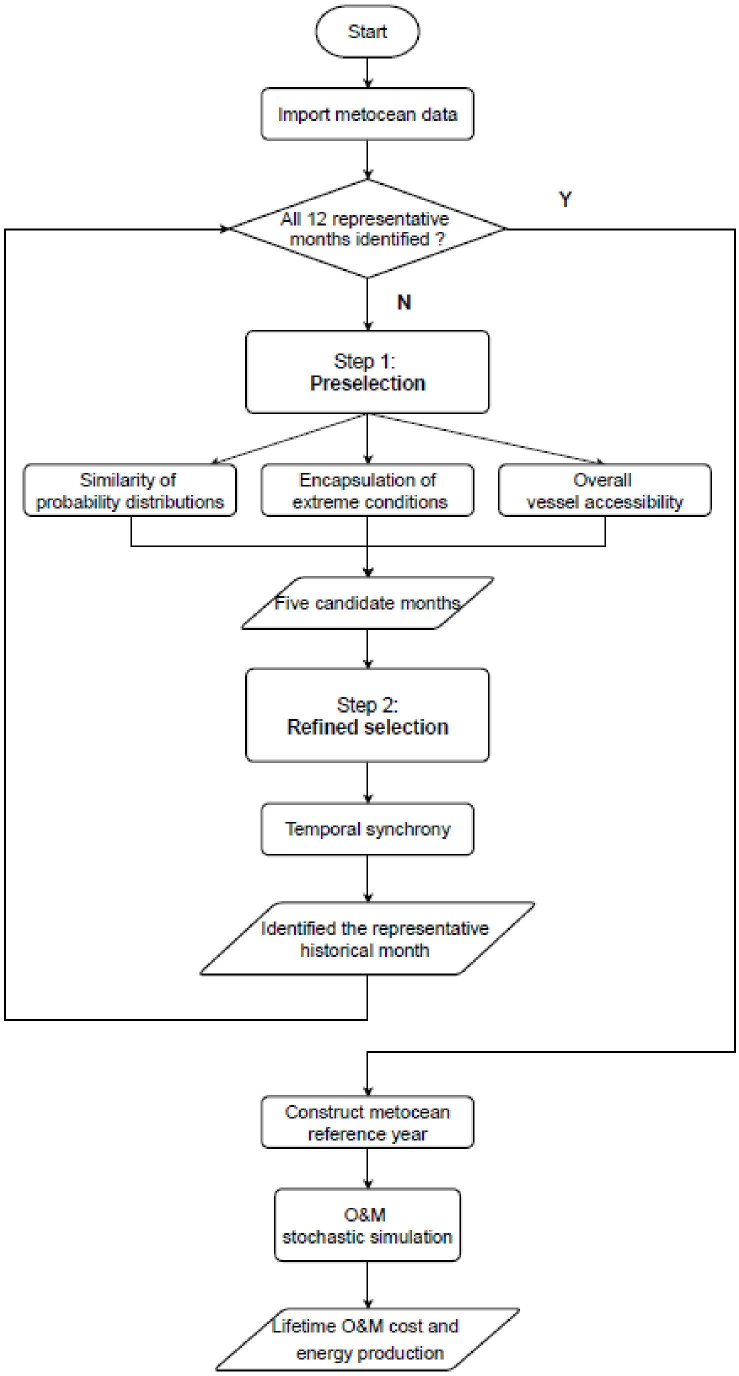

Figure 1. Schematic of the proposed hierarchical met-ocean data selection model.

A similar concept was used to generate a typical meteorological year (TMY) for building a performance simulation [38,39]. However, there are fundamental differences between our research and existing ones in terms of the nature of the targeted problem and the proposed method. To be specific, the O&M stochastic simulation imposes more stringent requirements on the synchrony of dynamic changes in temporal domain owing to its significant impact on vessel accessibility, maintenance cost, as well as energy generation. In addition, unlike the TMY model which is purely motivated to find the most average weather conditions, we propose a combination of distinct statistical components incorporating both average and extreme conditions to create a bespoke design of met-ocean reference year. The details of the proposed model are presented as below.

2.1. Preselection

The preselection aims to identify five candidate months from the long-term data set for each calendar month by examining the overarching distribution characteristics. Specifically, for each calendar month, an indicator of similarity between the individual historical month and the long-term met-ocean data belonging to the same calendar month is calculated. Three statistical measurements are incorporated in the similarity indicator, including the Jensen–Shannon (JS) divergence, the square of differences of extreme values and the difference in cumulative met-ocean windows. The first two components measure the similarities in terms of overall data distribution and coverage of harsh met-ocean conditions, whereas the last component measures the similarity of overall vessel accessibility.

The three components are combined by applying component weighting factors after normalisation to obtain a composite similarity score. For multivariate time series, the calculation of the three statistical components is conducted independently for each met-ocean parameter. An overall similarity score is derived by weighting the different parameters' respective similarity scores. As such, a holistic characterisation encompassing different aspects of met-ocean time series similarities is established and the individual historical months with higher similarities to the long-term met-ocean data are identified in the preselection stage.

2.1.1. Jensen-Shannon Divergence

The JS divergence is adopted to evaluate the closeness between the distribution of met-ocean data from a single historical month and the overall distribution constituted by all met-ocean data belonging to the same month. Jensen-Shannon (JS) divergence [37] is a statistical method of measuring the similarity between two probability distributions in comparison. It is the symmetrised and smoothed version of Kullback–Leibler (KL) divergence, which measures how a probability distribution diverges from a reference probability distribution as shown in Equations (1) and (2) [40]. JS divergence is chosen in this study owing to its capability of dealing with less-overlapped and non-overlapped distributions [41].

$$D_{JS}(P\,||\,Q) = \frac{1}{2}[D_{KL}(P\,||\,\frac{P+Q}{2}) + D_{KL}(Q\,||\,\frac{P+Q}{2})\,] \tag{1}$$

$$D_{KL}(P\,||\,Q) = \int \log\left(\frac{dP}{dQ}\right) dP \tag{2}$$

where D_{JS} and D_{KL} represent JS divergence and KL divergence, respectively. P and Q are two distributions of met-ocean data from a single historical month and from the long-term data belonging to the same calendar month. JS divergence scores are bounded by [0, 1], where smaller scores indicate higher similarities between distributions in comparison.

2.1.2. Encapsulation of Extreme Met-Ocean Conditions

In O&M analysis of ORE systems, extreme met-ocean conditions are critical due to their profound impacts on component reliability and vessel accessibility in real life [42–44]. Therefore, the second component in the preselection is dedicated to the encapsulation of extreme met-ocean conditions. Specifically, we first calculate the differences with respect to the maximum and minimum values between the two distributions in comparison, i.e., distributions from a single historical month and from the long-term data of the same calendar month, respectively. Then the sum of squares of the obtained differences is derived to indicate the coverage of extreme met-ocean conditions in comparison with the full spectrum, as shown in Equation (3).

$$C_{extreme} = (P_{max} - Q_{max})^2 + (P_{min} - Q_{min})^2 \tag{3}$$

where $C_{extreme}$ represents the indicator for the coverage of extreme met-ocean conditions. P_{max} and P_{min} denote the maximum and minimum values in P distribution. Similarly, Q_{max} and Q_{min} denote the maximum and minimum values in Q distribution.

2.1.3. Vessel Accessibility

Vessel accessibility plays a significant role in determining downtime and O&M costs for ORE systems [45,46]. Therefore, the third component in the preselection is dedicated to the measurement of vessel accessibility. Firstly, the cumulative durations of available weather windows regarding the mean vessel limits of wave, wind and current are calculated for the single historical month and for the set of all same calendar months, respectively. Then the obtained accessible duration from a single month is scaled up by multiplying the total number of that calendar month contained in the historical record. The difference between the two types of cumulative durations is hence calculated to represent the similarity of overall vessel accessibility.

$$A_{diff} = P_{count} n_{year} - Q_{count} \tag{4}$$

where A_{diff} and n_{year} represent the difference in overall vessel accessibility and the total number of a specific calendar months, respectively. P_{count} and Q_{count} denote the count of suitable weather windows for P and Q distributions, respectively.

2.1.4. Overall Similarity Score

The three distinct elements are subsequently normalised and aggregated by applying weighting factors to obtain a composite similarity score. When multiple variables are contained in met-ocean time series, the three statistical components are calculated for each variable independently. The resulted composite similarity scores are then weighted to obtain an overall similarity score as shown in Equations (5) and (8).

$$S_{com} = w_{c1} D_{JS} + w_{c2} C_{extreme} + w_{c3} A_{diff} \tag{5}$$

$$S_{overall} = \sum_{i=1}^{n} w_i S_{com\ i} \tag{6}$$

$$w_{c1} + w_{c2} + w_{c3} = 1 \tag{7}$$

$$\sum_{i=1}^{n} w_i = 1 \tag{8}$$

where S_{com} and $S_{overall}$ denote composite similarity score and overall similarity score, respectively. w_{c1}, w_{c2}, w_{c3} represent three component weighting factors for JS divergence, coverage of extreme met-ocean condition and overall vessel accessibility, respectively. In addition, w_i indicates the weighting factor for i-th variable in a multi-variate time series.

Overall, the preselection identifies promising candidate months with high distribution similarities to the long-term met-ocean data by comparing overall distributions, coverages of extreme met-ocean conditions, as well as overall vessel accessibility. Where the preselection has assessed the similarity of the distributions, the subsequent refined selection assesses the temporal patterns in the data.

2.2. Refined Selection

In addition to the distribution characteristics, the sequence of met-ocean data is also critical to the calculation of weather window. Therefore, in the refined selection, a statistical component is devised to measure the level of synchrony between met-ocean data sets in temporal domain and determines the most representative historical month from the preselected five candidates.

Temporal Synchrony

In O&M stochastic simulation, it is data sequence over consecutive timesteps that establishes suitable weather windows, not separate data points. The change of sequence within met-ocean data can have significant impacts on weather windows and vessel accessibility. Therefore, a refined selection process is developed focusing on the temporal change of met-ocean variables as time evolves. The similarity regarding the patterns of temporal changes between met-ocean time series is denoted as temporal synchrony. The candidate month which generates the highest synchrony score, as compared to the long-term met-ocean record, is considered as the most representative month.

To ensure the equal length between time series data in comparison, the means of long-term met-ocean data are calculated by averaging all monthly time series. This process is performed separately for each calendar month. Despite suffering from reduced variability, calculating averages of different periods is widely used for temporal aggregation in existing studies [30,47,48]. In this study, the averaging process is adopted for two considerations. Firstly, the purpose of the refined selection is to identify a historical month which can find the average of simulation results from using all data of that calendar month. This average enables us to estimate the lifetime O&M results effectively. Secondly, the means of time series is only used as a reference for the selection and the actual variability of met-ocean time series is still preserved in the identified representative data.

The first-order difference is then calculated to obtain the change between consecutive observations of a met-ocean variable. The cosine similarity is subsequently calculated using the derived first-order differences to evaluate the level of synchrony in terms of changes between met-ocean time series in comparison, as shown in Equations (9)–(11).

$$P_{diff}(t) = x(t) - x(t-1) \tag{9}$$

$$Q'_{diff}(t) = x'(t) - x'(t-1) \tag{10}$$

$$Co_{sim} = \frac{\sum_{t=1}^{n} P_{diff}(t) Q'_{diff}(t)}{\sqrt{\sum_{t=1}^{n} P_{diff}^{2}(t)} \sqrt{\sum_{t=1}^{n} Q'^{\,2}_{diff}(t)}} \tag{11}$$

where P_{diff} represents the first-order difference of the time series from a single historical month and Q'_{diff} denotes the first-order difference of the averaged long-term time series. In addition, Co_{sim} is cosine similarity for the two vectors of first-order difference. $x(t-1)$ and $x(t)$ indicate data instances at timestep $t-1$ and t in a single-month time series, whereas $x'(t-1)$ and $x'(t)$ represent data instances at timestep $t-1$ and t in the averaged long-term time series.

As such, in the refined selection the temporal changes of met-ocean variables are compared whereas the overall characteristics of the statistical distributions are examined in the preselection. The representative met-ocean reference year yielded by the proposed hierarchical model is employed to reduce the computational cost of O&M stochastic simulation.

3. Validation

We first evaluate the impacts of each devised statistical component on the selection of representative months. Then the proposed model is coupled with an O&M stochastic simulation tool to evaluate the performance of the generated representative met-ocean reference year. The trial-and-error approach is adopted to identify suitable weighting factors for the employed statistical components based on the simulation results.

The UNEXE O&M [49] tool is employed for the O&M stochastic simulation. The experimental settings are determined by following the existing study [2]. A representative floating offshore wind farm with five 9.5 MW wind turbines in Scotland is employed as a case study. Nine components with higher failure rates are considered for maintenance, including pitch and hydraulic system, generator, gearbox, blades, floating platform, mooring lines, anchors, inter-array cables and export cables. The reliability data for different components are obtained from the existing literature [50–53]. Four types of vessels are employed for undertaking various maintenance tasks, namely a crew transfer vessel (CTV), a field support vessel (FSV), a heavy-lift vessel (HLV), as well as an anchor handling tug supply (AHTS) vessel. The weather limits associated with each type of vessel are provided in Table 1. The met-ocean data set with twenty historical years is employed for the case study, i.e., spanning from 1995 to 2014. The variables contained in the data set include significant wave height, peak period, direction at peak spectral, wind speed, wind direction, current speed and current direction. They are measured at an interval of 3 h. A total number of 100 runs is deployed in the Monte Carlo simulation based on the existing study [2]. All experiments were conducted on a machine with 2.30 GHz 4-core CPU and 32 GB RAM. It should be noted that the focus of this research is to investigate the performance of the selected representative met-ocean data, rather than providing actual guidance on O&M strategy.

Table 1. Weather limits of the employed vessels.

Name of the Vessel	CTV	FSV	HLV	AHTS
Wave height limit, [m]	2.5	1.8	1.5	3
Wind speed limit [m/s]	30	30	25	30
Current speed limit [m/s]	5	5	4	4

3.1. Impacts of the Devised Statistical Components

In order to avoid the disturbance imposed by other statistical components, the impacts of each component are investigated separately by switching off the irrelevant ones, i.e., setting weighting factors as 0. For the benefit of comparison, the results of March are used as an example to illustrate the distinctive effects driven by different components. The cumulative distributions and probability densities of significant wave height in March from the five candidate years identified by the three statistical components, i.e., the JS divergence, the extreme condition encapsulation and the overall vessel accessibility, are illustrated in Figures 2–4, respectively.

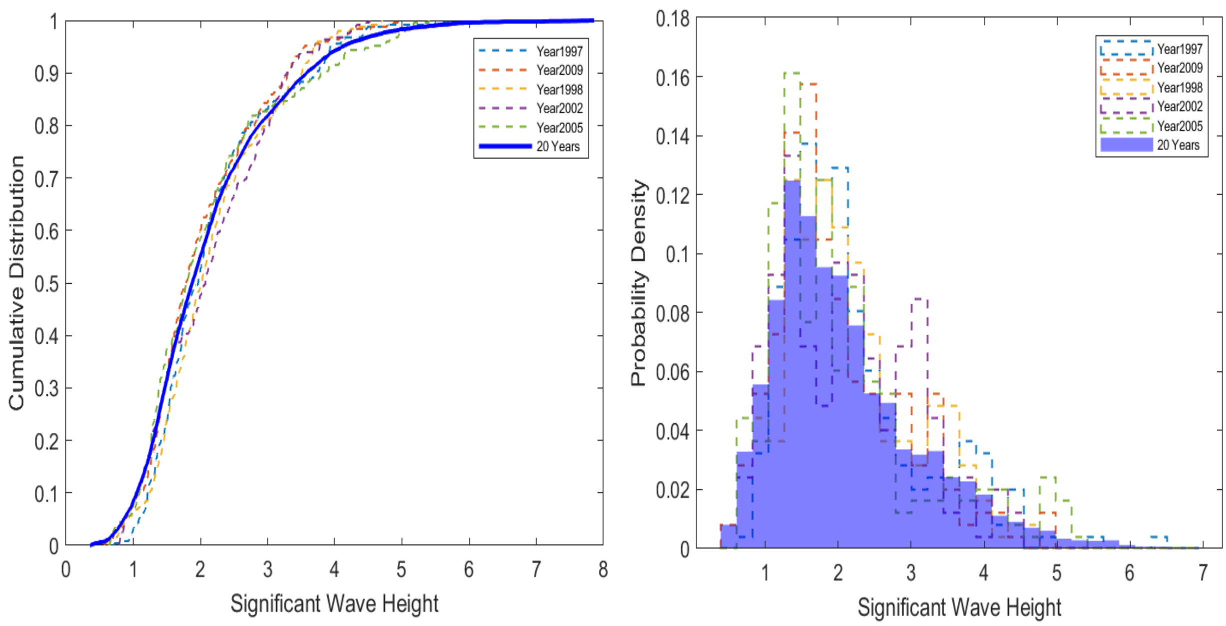

Figure 2. The cumulative distributions (**left**) and probability densities (**right**) of the significant wave height in March from five candidate months yielded by the component of JS divergence.

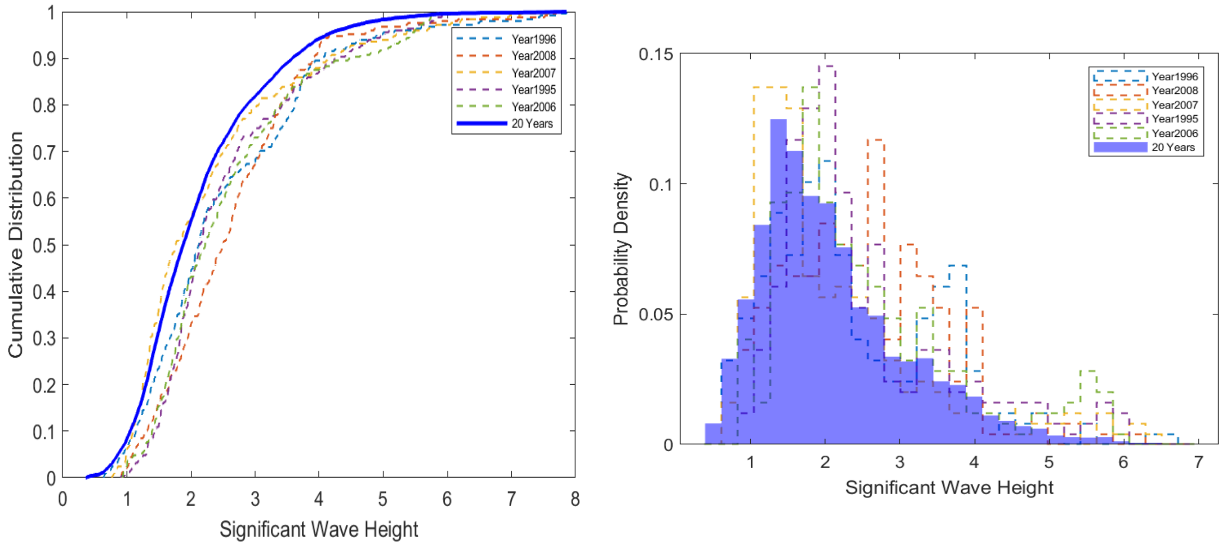

Figure 3. The cumulative distributions (**left**) and probability densities (**right**) of significant wave height in March from five candidate months identified by the component of extreme condition encapsulations.

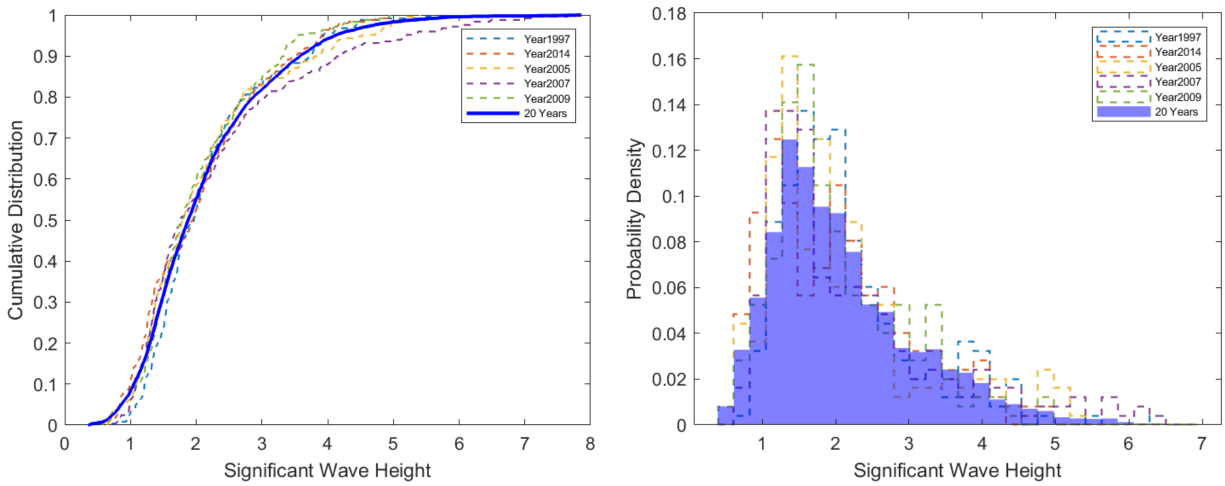

Figure 4. The cumulative distributions (**left**) and probability densities (**right**) of significant wave height in March from five candidate months yielded by the component of vessel accessibility.

With respect to the JS divergence, the resulted five candidate months for March, i.e., 1997, 1998, 2002, 2005 and 2009 as illustrated in dash lines in Figure 2, possess very similar distributions to that of the twenty-year case. They enclose the distribution of the twenty-year met-ocean data with narrow gaps across the whole spectrum of the significant wave height. This resemblance demonstrates the efficacy of the JS divergence in capturing characteristics of overall distributions of time series.

With respect to the extreme condition encapsulations, the yielded five candidate months for March, i.e., 1995, 1996, 2006, 2007 and 2008 as illustrated in dash lines in Figure 3, are able to fully cover the harsh met-ocean conditions contained in the twenty-year met-ocean data, as evidenced by the higher probability densities of the candidates in regions with large significant wave heights. However, discrepancies in the overall distribution landscapes can be observed from the candidate months in comparison with the twenty-year case.

With respect to the overall vessel accessibility, the identified five candidate months for March, i.e., 1997, 2005, 2007, 2009 and 2014 as illustrated in dash lines in Figure 4, demonstrate a high level of resemblance to the twenty-year case when the significant wave heights are below the mean value of vessel limits, i.e., 2.2 m. With the further increase in significant wave heights, the divergence of distributions becomes larger. This is due to the specified emphasis on the met-ocean data which comply with vessel limits, e.g., the significant wave height is lower than the defined threshold of vessel limits, in order to evaluate the overall vessel accessibility.

With respect to the temporal synchrony, the identified representative month (red curve in Figure 5) demonstrates identical granular changes to the twenty-year case (denoted as the blue curve in Figure 5) in the temporal domain. A close match of major peaks and troughs between the identified typical year and the twenty-year scenario can be observed in Figure 5. The variability in the twenty-year case is smaller than the selected representative year due to the fluctuations being reduced by averaging significant wave heights from twenty historical years. However, the essence of measuring temporal synchrony is to compare the change patterns of met-ocean conditions, rather than matching exact values. In short, the effectiveness of the devised component of temporal synchrony is verified by the identical change in patterns shared by the representative data and the twenty-year data set.

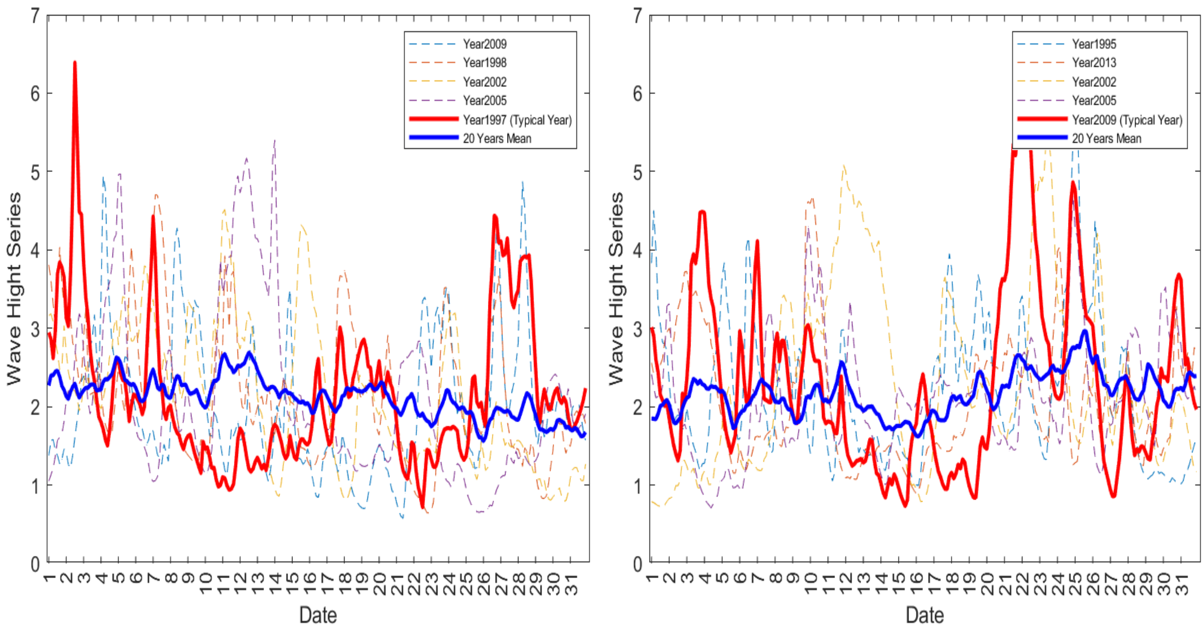

Figure 5. The significant wave height time series of March (**left**) and October (**right**) from the most representative years identified by the component of temporal synchrony.

3.2. Parameter Tuning

In the proposed statistical model, two types of weighting factors exist, including parameter weighting factors and component weighting factors. In this case study, two met-ocean parameters, namely significant wave height and wind speed, are considered and assigned with an equal weighting factor of 0.5 since they are commonly used for assessing vessel accessibility [2,54]. The major attention is dedicated to the tuning of parameters for the three statistical components in the preselection. Based on the analysis of impacts from individual components, the most effective combination of them is identified by devising bespoke weighting factors through a trial-and-error process.

A heuristic search process is conducted to identify the most effective weighting factors with efficiency. The JS divergence and overall vessel accessibility are prioritised to start the tuning process owing to their capability of selecting the representative months with similar distributions to the twenty-year data set, as shown in Figures 2 and 4. The identified elite solution of weighting factors is then further improved by manipulating the level of participation for the component of extreme met-ocean encapsulation. The search space between [0,1] is investigated to enable different combinations of components of JS divergence and overall vessel accessibility. Both the O&M cost and the energy production results are employed to evaluate the fitness of weighting factor solutions, as compared against the results from using the twenty-year met-ocean data set.

The empirical results of O&M cost and energy production are presented in Table 2. When applying the equal weighting factor of 0.5 for the components of JS divergence and extreme condition encapsulation, the simulation results demonstrate small variances to the twenty-year case, i.e., −4.83% for the lifetime O&M cost and 3.83% for the lifetime energy production. Moreover, a better combination of weighting factors is identified by allowing a modest participation for the component of extreme condition encapsulation. Specifically, by applying the weighting factors of (0.4, 0.1, 0.5) for the components of JS divergence, encapsulation of extreme met-ocean conditions and overall vessel accessibility, the best simulation results with the least variances to the twenty-year case are obtained, i.e., −4.83% for the lifetime O&M cost and 3.14% for the lifetime energy production. The resulted met-ocean reference year incorporates the following twelve representative calendar months, i.e., January in 2003, February in 2001, March in 1997, April in 1999, May in 2003, June and July in 2001, August in 2007, September in 2001, October in 2009, November in 2007 and December in 2008.

Table 2. O&M simulation results from the representative met-ocean reference year yielded by different combinations of component weighting factors.

Weights (w_{c1}, w_{c2}, w_{c3})	O&M Cost (m£)	O&M Cost Scaled (m£)	Variations of O&M Cost	Energy Production (MWh)	Energy Production Scaled (MWh)	Variations of Energy Production
20-year data	86.16	86.16		4.336×10^6	4.336×10^6	
(1, 0, 0)	3.57	71.40	−17.13%	2.275×10^5	4.551×10^6	4.96%
(0, 1, 0)	3.70	74.00	−14.11%	2.401×10^5	4.802×10^6	10.75%
(0, 0, 1)	3.68	73.60	−14.58%	2.259×10^5	4.518×10^6	4.21%
(0.8, 0, 0.2)	3.57	71.40	−17.13%	2.284×10^5	4.567×10^6	5.34%
(0.6, 0, 0.4)	4.10	82.00	−4.83%	2.267×10^5	4.534×10^6	4.59%
(0.5, 0, 0.5)	4.10	82.00	−4.83%	2.251×10^5	4.502×10^6	3.83%
(0.4, 0, 0.6)	4.10	82.00	−4.83%	2.270×10^5	4.540×10^6	4.70%
(0.2, 0, 0.8)	3.68	73.60	−14.58%	2.313×10^5	4.627×10^6	6.71%
(0.4, 0.1, 0.5)	4.10	82.00	−4.83%	2.236×10^5	4.472×10^6	3.14%
(0.4, 0.2, 0.4)	3.69	73.80	−14.35%	2.240×10^5	4.479×10^6	3.31%
(0.3, 0.4, 0.3)	3.69	73.80	−14.35%	2.271×10^5	4.542×10^6	4.76%
(0.2, 0.6, 0.2)	3.70	74.00	−14.11%	2.304×10^5	4.609×10^6	6.30%
(0.1, 0.8, 0.1)	3.71	74.20	−13.88%	2.401×10^5	4.802×10^6	10.77%

Moreover, the simulation results from different combinations of weighting factors indicate the complexity of the problem. To be specific, the relationships between the weighting factors and the results of the O&M costs and energy productions are nonlinear, as evidenced by the empirical results. The increase in the weighting factor for any specific statistical component does not guarantee a continuous increase or decrease in the accuracy of the simulated O&M costs and energy productions. This also indicates that the impacts of met-ocean data on the simulated stochastic outputs are sophisticated. The selection of suitable met-ocean data for O&M assessment is not an easy task owing to the large search space. The total number of solutions in a 20-year case is 4.096×10^{15}, i.e., 20^{12}. However, according to the results of the parameter tuning, good performances can be obtained when similar weights are assigned to the components of JS divergence and vessel accessibility and the weights for the component of extreme conditions are kept small, such as (0.6, 0, 0.4), (0.5, 0, 0.5), (0.4, 0, 0.6), (0.4, 0.1, 0.5). These four combinations of weighting factors achieved the most accurate O&M cost results with a deviation of 4.83% from the 20-year case. Despite resulting in the same O&M costs, the met-ocean reference years generated by these four weighting solutions are not entirely the same and different historical data are selected on several calendar months, as shown in Table 3.

Table 3. The representative met-ocean reference years identified by four different combinations of component weighting factors.

Weights (w_{c1}, w_{c2}, w_{c3})	Jan	Feb	Mar	Apr	May	Jun	Jul	Aug	Sep	Oct	Nov	Dec
(0.6, 0, 0.4)	2008	2001	1997	1999	2003	2003	2001	2007	2001	2009	2001	2008
(0.5, 0, 0.5)	2003	2001	1997	1999	2003	1995	2001	2007	2001	2009	2001	2008
(0.4, 0, 0.6)	2003	2001	1997	1999	2003	2001	2001	2007	2001	2009	2001	2008
(0.4, 0.1, 0.5)	2003	2001	1997	1999	2003	2001	2001	2007	2001	2009	2007	2008

Overall, a heuristic solution of weighting factors is identified where the four statistical components, i.e., the JS divergence, the extreme condition encapsulation, the overall vessel accessibility, as well as the temporal synchrony, complement each other to attain the refined representation of realistic met-ocean conditions. The resulted representative met-ocean data set is able to emulate the original simulation results from using twenty-year met-ocean data with small variations on the test scenario with five turbines.

4. Results

A comprehensive evaluation was conducted for the proposed data selection model equipped with the identified most effective weighting factors, i.e., 0.4, 0.1, and 0.5 for the components of JS divergence, extreme condition encapsulation and vessel accessibility, respectively. Three performance indicators are examined in detail, including computational time, O&M cost and energy production. Five wind farm sizes are tested: i.e., 2, 5, 10, 20, 30 wind turbines.

4.1. Simulation Results for Different Wind Farm Configurations

As shown in Table 4, the results are the averages based on 100 independent runs in the Monte Carlo simulation. The simulation results obtained from the single-year representative met-ocean data are multiplied by the total number of years, i.e., 20, to generate synthetic lifetime results. Across the tested five wind farm sizes, the selected representative met-ocean reference year is capable of emulating the lifetime results of the twenty-year case with small deviations.

Table 4. O&M simulation results of different wind farm configurations using 20-year and representative met-ocean data.

Met-Ocean Data Set	Configuration	Computation Time (s)	Reduction of Computation Time	O&M Cost (m£)	Variations of O&M Cost	Energy Production (MWh)	Variations of Energy Production
20-year	2	15,745.8		34.30		1.735×10^6	
Representative	2	568.0	96.39%	35.60	3.79%	1.787×10^6	2.99%
20-year	5	21,405.2		86.16		4.336×10^6	
Representative	5	703.3	96.71%	82.00	−4.83%	4.472×10^6	3.14%
20-year	10	68,514.8		173.06		8.671×10^6	
Representative	10	2868.9	95.81%	173.00	−0.03%	8.890×10^6	2.53%
20-year	20	178,241.7		345.34		1.734×10^7	
Representative	20	4183.6	97.65%	337.40	−2.30%	1.787×10^7	3.07%
20-year	30	297,086.5		515.87		2.601×10^7	
Representative	30	7700.4	97.41%	502.20	−2.65%	2.679×10^7	3.00%

Specifically, with respect to the O&M cost, the absolute variations are within 5%, i.e., from 0.03% to 4.83% across different configuration scenarios, between the two types of met-ocean data. The highest variation occurs in the scenario of five wind turbines and the lowest variation occurs in the scenario of ten turbines. In comparison, the results of energy production demonstrate a smaller range of variances across different wind farm configurations, i.e., from 2.53% to 3.14%. Similarly, the scenarios where the highest and lowest variations occur for the energy production are identical to those of the O&M cost, i.e., five and ten turbines, respectively.

In addition to the simulation results, the computational efficiency is also compared for two types of met-ocean data. As shown in Table 4, using the representative met-ocean reference data, the computation time of O&M simulation is reduced significantly, i.e., from 95.81% to 97.65% across five configuration scenarios, in comparison with using the twenty-year met-ocean data. In other words, the simulation speed becomes 28, 30, 24, 43 and 39 times faster on the five scenarios, respectively. This indicates that the computational efficiency can be boosted massively by employing the representative met-ocean data.

Furthermore, the performances of the met-ocean reference year are compared against three baseline individual years chosen at different timepoints, i.e., the beginning (year 1995), the midpoint (year 2004), and the end (year 2014), as shown in Table 5. Evaluated using the wind farm with five turbines, the met-ocean reference year demonstrates much smaller variations on the results of the lifetime O&M costs and energy productions than the three baseline years. More specifically, with respect to the O&M costs, the deviations demonstrated by the baseline years of 1995, 2004 and 2014 are 11.6%, 8.8%, 10.4% larger than the met-ocean reference year, respectively. With respect to the energy productions, the deviations of three baseline years are 3.43%, 3.18% and 5.46% higher than the met-ocean reference year. As a result, the generated representative met-ocean reference can achieve more accurate simulation results than single historical years.

Table 5. O&M simulation results of the met-ocean reference year and the baseline individual years.

Met-Ocean Data Set	Configuration	Computation Time (s)	Reduction of Computation Time	O&M Cost (m£)	Variations of O&M Cost	Energy Production (MWh)	Variations of Energy Production
20-year	5	21,405.2		86.16		4.336×10^6	
Reference year	5	703.3	96.71%	82.00	−4.83%	4.472×10^6	3.14%
Year 1995	5	667.2	96.88%	72.00	−16.43%	4.620×10^6	6.57%
Year 2004	5	672.7	96.78%	74.40	−13.65%	4.610×10^6	6.32%
Year 2014	5	649.4	96.88%	73.00	−15.27%	4.708×10^6	8.60%

Based on the empirical results, the representative met-ocean reference data set is able to reduce the computation time of the O&M stochastic simulation significantly while emulating the original simulation results with minor deviations. As such, a trade off between computational efficiency and model fidelity can be attained and the practicality of the O&M stochastic simulation can be enhanced considerably.

4.2. Construction of Distributions for Lifetime Performance Indicators

In addition to the average results, the distributions of simulation outputs are also preferred in order to understand variability of performance indicators with respect to complex uncertainties embedded in the O&M stochastic simulation [2]. In this section, the distributions of the lifetime O&M cost and energy production are established for the representative met-ocean data, using the results pool generated by 100 runs in the Monte Carlo simulation. Specifically, random sampling with replacement is employed to draw 20 samples from the result pool, representing simulation results from twenty individual years. These samples are subsequently aggregated to produce a synthetic instance pertaining to a specific lifetime outcome, such as the lifetime O&M cost or the lifetime energy production. The above procedures are repeated to generate 100 synthetic instances, signifying 100 independent runs as prescribed in the Monte Carlo simulation. The distributions of lifetime performance indicators are thereafter established for the representative met-ocean data and compared against those resulted from using the twenty-year met-ocean data.

As shown in Figure 6, the histograms for the 20-year case and the representative year are highlighted in orange and blue colours, respectively, whereas the red curves denote the fitted probability density functions based on the histograms. The constructed distributions of the lifetime O&M cost for the representative met-ocean reference year demonstrate high similarities to those yielded by the twenty-year met-ocean data. More specifically, the two types of distributions exhibit identical patterns characterised by predominant overlaps and homogeneous spectrums. This similarity can be observed across different configuration scenarios. Furthermore, the Wilcoxon rank sum test is conducted to provide statistical evidence regarding the level of distinctiveness between two distributions in comparison. The rank sum test results are higher than 0.05 for all tested configuration scenarios, i.e., 1.89×10^{-1}, 9.58×10^{-1}, $1.53 \times 10^{-1}$and 9.39×10^{-2} for 5, 10, 20 and 30 wind turbines, respectively, as shown in Table 6. As a result, the hypothesis that two distributions are likely to be derived from the same population cannot be rejected. As such, the original lifetime O&M cost distributions can be reproduced with a high level of confidence by using the representative met-ocean reference year, as evidenced by the results of the statistical test and different configuration scenarios.

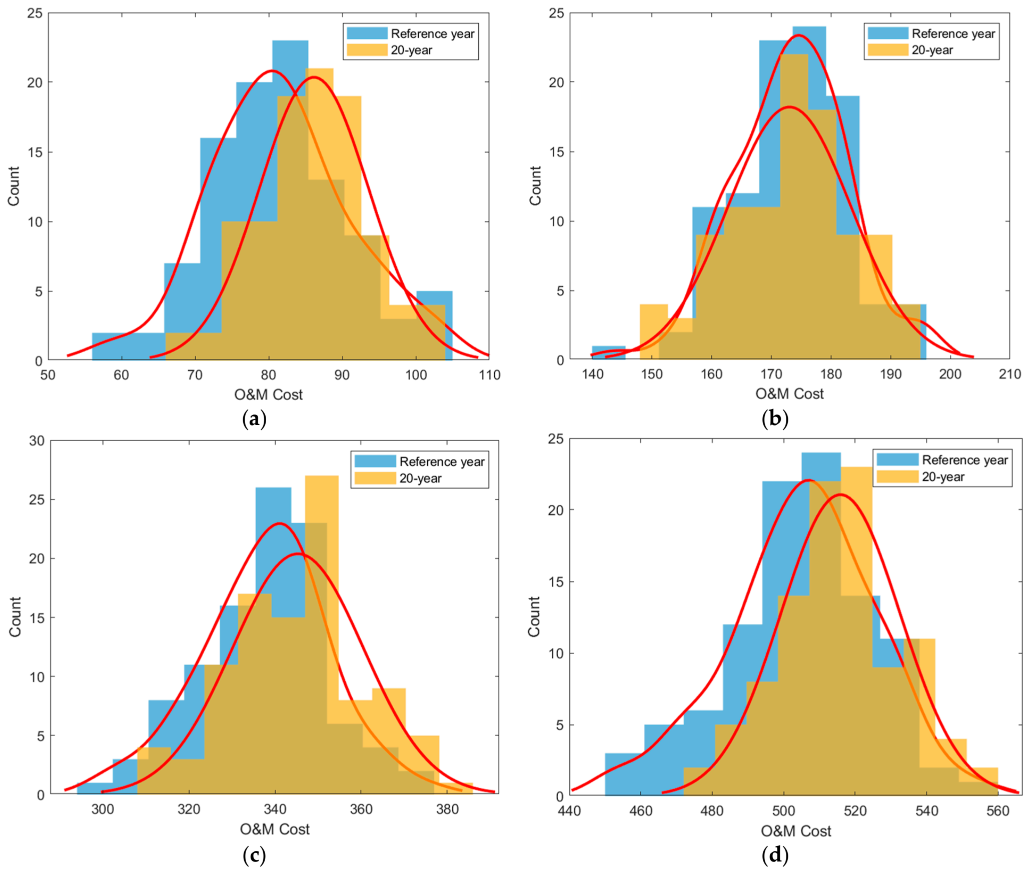

Figure 6. The lifetime O&M cost distributions resulted from the representative met-ocean reference year and twenty-year met-ocean data for (**a**) 5 turbines, (**b**) 10 turbines, (**c**) 20 turbines, (**d**) 30 turbines.

Table 6. Wilcoxon rank sum test results for lifetime O&M cost and lifetime energy production.

Met-Ocean Data Set	Wilcoxon Rank Sum Test Results			
O&M cost	1.89×10^{-1}	9.58×10^{-1}	1.53×10^{-1}	9.39×10^{-2}
Energy Production	1.18×10^{-9}	6.20×10^{-8}	1.48×10^{-17}	4.42×10^{-24}

The distributions are also constructed for the lifetime energy production for different configuration scenarios, as shown in Figure 7. The red curves are the fitted probability density functions based on the histograms. The two distributions resulted from two types of met-ocean data exhibit a higher level of distinctiveness in their spectrums, hence leading to a lower level of overlaps. The lifetime energy production results of the representative met-ocean reference year appear to be slightly overestimated compared to those of the twenty-year met-ocean data. This distinctiveness is also verified by the rank sum test results below the threshold of 0.05, i.e., 1.18×10^{-9}, 6.20×10^{-8}, 1.48×10^{-17} and 4.42×10^{-24} for 5, 10, 20 and 30 wind turbines, respectively, as shown in Table 4. This overestimation of the lifetime energy production could be attributed to the underestimation of failure occurrence and downtime on certain components. Using blades as an example, for the configuration scenario of five turbines, the total number of blade failures and the resulted downtime for the representative met-ocean data are 8.69% and 7.35% less, respectively, than those of the twenty-year case. Nevertheless, the variances between the two distributions are small in comparison with the scales of the lifetime energy production. The relative differences of mean values of the two distributions are 3.14%, 2.40%, 3.03%, 2.97% for the configuration scenarios of 5, 10, 20, 30 turbines, respectively. Therefore, the constructed distributions of the lifetime energy production are effective in providing reliable estimations regarding the energy yield of ORE systems.

Overall, the representative met-ocean reference year identified by the proposed hierarchical data selection model is able to emulate both the average results and distributions pertaining to the lifetime performance indicators, e.g., the lifetime O&M cost and the lifetime energy production. More importantly, the empirical results indicate that the computation time can be reduced by up to 97.65% and the simulation speed becomes 43 times faster. Therefore, the proposed data selection model is capable of achieving the advanced trade off between the computational cost and the model fidelity, hence enhancing the practicality of the O&M stochastic simulation significantly.

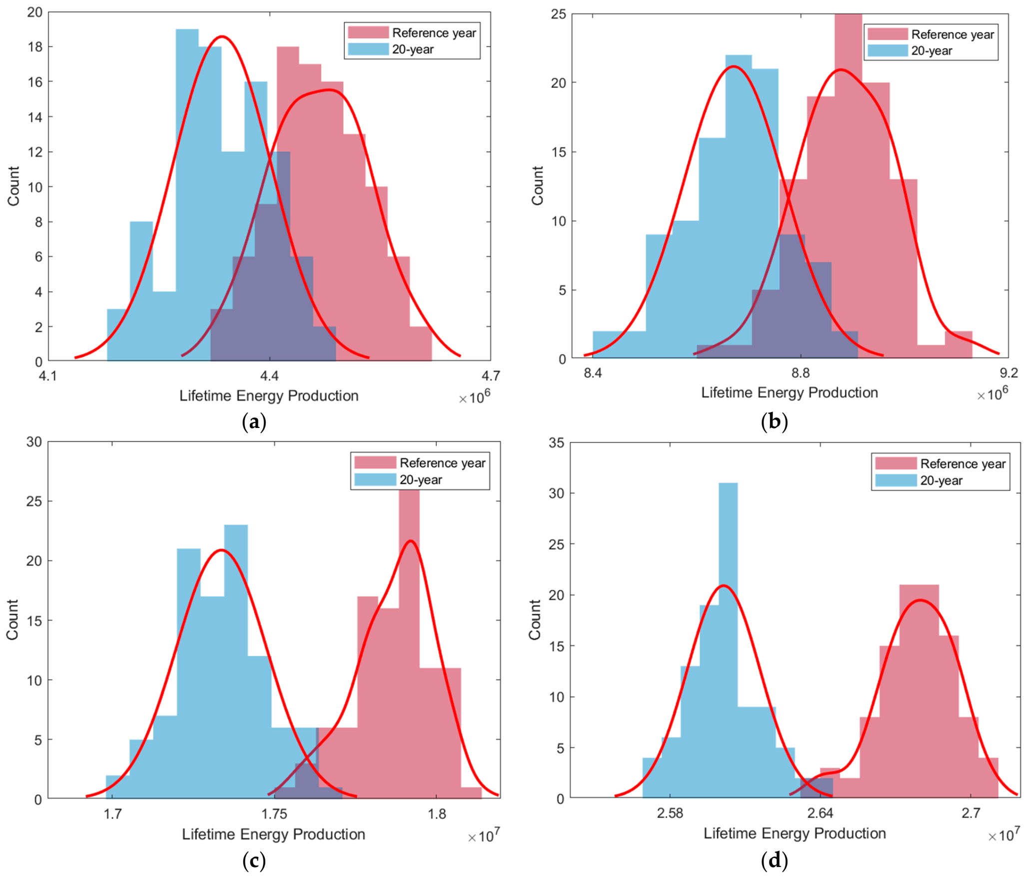

Figure 7. The lifetime energy production distributions resulted from the representative met-ocean reference year and twenty-year met-ocean data for (**a**) 5 turbines, (**b**) 10 turbines, (**c**) 20 turbines, (**d**) 30 turbines.

5. Discussion

Despite following a similar two-step hierarchical structure, our proposed model employs distinctive statistical measurements to account for the unique characteristics in the domain of O&M stochastic simulation, compared to the data selection model applied in the domain of dynamic building simulation [55–57]. More specifically, in O&M stochastic analysis, dynamic changes of met-ocean conditions play a significant role in affecting O&M cost and energy production owing to its impact on the availability of a suitable weather window for maintenance operations [58]. Therefore, in the refined selection of the proposed model, temporal synchrony is measured by calculating the cosine similarity using the first difference to capture dynamic changes in the temporal domain. In contrast, the data selection model employed in the dynamic building simulation only considers spatial proximity of time series by calculating the root mean square error (RMSE), which ignores time dependency embedded in the time series data and cannot satisfy the stringent requirement in the O&M stochastic simulation.

We validate the above argument by further conducting a comparison experiment, where the cosine similarity is replaced by RMSE for the selection of representative data. The yielded met-ocean reference year is then employed for the O&M simulation and the lifetime performance indicators are calculated. In comparison with the twenty-year case, the variations for the lifetime O&M cost and energy production are −17.13% and 4.19%, respectively, which are much higher than the results yielded by using the component of temporal synchrony, i.e., −4.83% and 3.14% for the lifetime O&M cost and the energy production, respectively.

Furthermore, the decomposed results with respect to component failures and downtime are presented in Table 7 for comparison between using the devised temporal synchrony component, i.e., cosine similarity, and the spatial proximity indicator, i.e., RMSE. Despite the identical outcomes of failure occurrence for the considered seven major wind turbine components, large variances can be observed between the results of downtime yielded by the two statistical measurements. Specifically, the downtime results induced by cosine similarity are much closer to the original twenty-year case than those induced by RMSE, across all major components. As an example, with respect to the downtime caused by the failures of mooring lines, the variances for the two methods of cosine similarity and RMSE are −0.57% and 18.93%, respectively, as compared against the twenty-year scenario. This relative difference in mooring lines alone between two methods amounts to 714 h in terms of absolute downtime. Such evident disparities in the downtime results can be ascribed to the failure of extracting dynamic changes in met-ocean conditions in the temporal domain when using RMSE as the selection criteria in the refined selection. In contrast, the devised component of temporal synchrony enables the identified representative met-ocean data to emulate the granular and continuous changes in a realistic met-ocean environment, therefore obtaining better simulation results with high fidelities.

Table 7. The number of failure occurrences and the system downtime over the 20-year lifetime for the proposed model where cosine similarity is employed and for a test model where RMSE is considered in the refined selection.

Major Components	Results of Failure Occurrence					Results of Downtime				
	20-Year	Cosine Similarity		RMSE		20-Year	Cosine Similarity		RMSE	
Floating platform	29.4	29.2	−0.68%	29.2	−0.68%	492.0	462.8	−5.93%	446.2	−9.31%
Mooring lines	17.8	17.4	−2.36%	17.8	−0.11%	3891.0	3869.0	−0.57%	4627.4	18.93%
Anchors	19.8	16.6	−16.12%	16.6	−16.12%	4155.0	3026.0	−27.17%	2841.6	−31.61%
Pitch and Hydraulic	32.8	33.0	0.76%	33.0	0.76%	15,988.0	12,961.4	−18.93%	11,354.0	−28.98%
Generator	29.6	27.0	−8.85%	27.0	−8.85%	1820.0	1572.0	−13.63%	1570.0	−13.74%
Gearbox	18.4	19.4	5.21%	19.8	7.38%	886.0	873.0	−1.47%	804.2	−9.23%
Blades	16.0	14.6	−8.69%	14.6	−8.69%	588.0	544.8	−7.35%	504.2	−14.25%

6. Conclusions

In this research, a hierarchical data selection model has been proposed to reduce the computational cost of an O&M stochastic simulation and achieve fast evaluation for ORE systems. The proposed model includes two steps, namely the preselection and the refined selection, to establish a fine representation of met-ocean conditions from large volumes of met-ocean time series data. The preselection employs three distinctive statistical components, i.e., the JS divergence, the encapsulation of extreme met-ocean conditions, as well as the overall vessel accessibility, to emulate holistic distribution characteristics embedded in the original met-ocean time series. In the refined selection, the component of temporal synchrony is devised to mirror the dynamic changes of met-ocean conditions in the temporal domain. As such, the proposed hierarchical model is capable of establishing a comprehensive description of realistic met-ocean conditions by incorporating different features, including probability distribution, extreme sample points, local information regarding vessel limits, as well as granular temporal changes.

A met-ocean reference year comprising twelve representative historical months is generated by the proposed model and subsequently employed as the input data set in the O&M stochastic simulation. Evaluated using a floating offshore wind farm with five capacity scenarios, i.e., 2, 5, 10, 20, 30 turbines, the yielded representative met-ocean reference year reduces computational cost of the O&M simulation by up to 97.65%. The simulation speed is therefore 43 times faster compared to using the twenty-year met-ocean data. Moreover, the distributions of synthetic lifetime O&M cost and energy production are constructed for the representative met-ocean reference year for further comparison. Evidenced by the Wilcoxon rank sum test, the original lifetime O&M cost distributions yielded by the twenty-year met-ocean data set are reproduced vividly by the representative met-ocean data. Minor deviations can be observed between the distributions of lifetime energy production from two types of met-ocean files, but the relative differences of the means are small. Therefore, the representative met-ocean reference year is able to emulate the original simulation results with a high level of confidence. An advanced trade off between computational efficiency and model fidelity can be attained by the proposed hierarchical met-ocean data selection model for the O&M stochastic simulation. Overall, the four devised statistical components in collaboration account for the efficacy of the proposed model by establishing a fine representation of realistic met-ocean conditions both in overall distributions and in temporal changes.

For future research, thorough comparisons between our proposed model and the conventional method will be conducted on detailed metrics, such as weather delays, using more case studies to gain better understandings about the deviations of the simulated results and to further improve the data selection mechanism. In addition, the proposed model will be integrated with optimisation algorithms to automatically identify the optimal settings of weighting factors for different components and achieve a higher level of intelligence and automation for undertaking complex modelling problems of ORE systems [15,59–63].

Author Contributions: Conceptualization, H.X. and L.J.; Methodology, H.X. and L.J.; Software, H.X.; Validation, H.X.; Formal Analysis, H.X.; Investigation, H.X.; Resources, L.J.; Data Curation, H.X.; Writing—Original Draft Preparation, H.X.; Writing—Review and Editing, L.J.; Visualization, H.X.; Supervision, L.J.; Project Administration, L.J.; Funding Acquisition, L.J. All authors have read and agreed to the published version of the manuscript.

Funding: This study has received funding through the project "Cornwall FLOW Accelerator" funded by European Regional Development Fund (ERDF), grant no. 115535.

Data Availability Statement: Publicly available datasets were analyzed in this study. This data can be found here: https://marendata.eu.

Conflicts of Interest: The authors declare no conflict of interest.

Nomenclature

O&M	Operation and Maintenance
ORE	Offshore Renewable Energy
MCMC	Markov Chains Monte Carlo
TMY	Typical Meteorological Year
JS	Jensen-Shannon
KL	Kullback-Leibler
CTV	Crew Transfer Vessel
FSV	Field Support Vessel
HLV	Heavy-Lift Vessel
AHTS	Anchor Handling Tug Supply
RMSE	Root Mean Square Error
D_{JS}	Jensen-Shannon divergence
D_{KL}	Kullback-Leibler divergence
P	Distribution of met-ocean data from a single historical month
Q	Distribution of met-ocean data from the long-term record
$C_{extreme}$	Coverage of extreme met-ocean conditions
P_{max}	Maximum value in P distribution
P_{min}	Minimum value in P distribution
Q_{max}	Maximum value in Q distribution
Q_{min}	Minimum value in Q distribution
A_{diff}	Difference of overall vessel accessibility
n_{year}	Total number of years in the met-ocean record
P_{count}	Count of suitable weather windows in P distribution
Q_{count}	Count of suitable weather windows in Q distribution
S_{com}	Composite similarity score
$S_{overall}$	Overall similarity score
w_{c1}	Weighting factor for JS divergence
w_{c2}	Weighting factor for coverage of extreme met-ocean condition
w_{c3}	Weighting factor for overall vessel accessibility
Co_{sim}	Cosine similarity for two vectors of first-order difference
P_{diff}	First-order difference of time series from a single month
Q'_{diff}	First-order difference of the averaged long-term time series

References

1. Garcia-Teruel, A.; Rinaldi, G.; Thies, P.R.; Johanning, L.; Jeffrey, H. Life cycle assessment of floating offshore wind farms: An evaluation of operation and maintenance. *Appl. Energy* **2022**, *307*, 118067. [CrossRef]
2. Rinaldi, G.; Garcia-Teruel, A.; Jeffrey, H.; Thies, P.R.; Johanning, L. Incorporating stochastic operation and maintenance models into the techno-economic analysis of floating offshore wind farms. *Appl. Energy* **2021**, *301*, 117420. [CrossRef]
3. Wang, L.; Zhao, T.; Lin, M.; Li, H. Towards realistic power performance and techno-economic performance of wave power farms: The impact of control strategies and wave climates. *Ocean Eng.* **2022**, *248*, 110754. [CrossRef]
4. Xu, X.; Robertson, B.; Buckham, B. A techno-economic approach to wave energy resource assessment and development site identification. *Appl. Energy* **2020**, *260*, 114317. [CrossRef]
5. Johnstone, C.M.; Pratt, D.; Clarke, J.A.; Grant, A.D. A techno-economic analysis of tidal energy technology. *Renew. Energy* **2013**, *49*, 101–106. [CrossRef]
6. Segura, E.; Morales, R.; Somolinos, J.A.; López, A. Techno-economic challenges of tidal energy conversion systems: Current status and trends. *Renew. Sustain. Energy Rev.* **2017**, *77*, 536–550. [CrossRef]
7. Franco, B.A.; Baptista, P.; Neto, R.C.; Ganilha, S. Assessment of offloading pathways for wind-powered offshore hydrogen production: Energy and economic analysis. *Appl. Energy* **2021**, *286*, 116553. [CrossRef]
8. Lucas, T.R.; Ferreira, A.F.; Santos Pereira, R.B.; Alves, M. Hydrogen production from the WindFloat Atlantic offshore wind farm: A techno-economic analysis. *Appl. Energy* **2022**, *310*, 118481. [CrossRef]
9. Babarit, A.; Gilloteaux, J.-C.; Clodic, G.; Duchet, M.; Simoneau, A.; Platzer, M.F. Techno-economic feasibility of fleets of far offshore hydrogen-producing wind energy converters. *Int. J. Hydrogen Energy* **2018**, *43*, 7266–7289. [CrossRef]
10. Röckmann, C.; Lagerveld, S.; Stavenuiter, J. Operation and Maintenance Costs of Offshore Wind Farms and Potential Multi-use Platforms in the Dutch North Sea. In *Aquaculture Perspective of Multi-Use Sites in the Open Ocean: The Untapped Potential for Marine Resources in the Anthropocene*; Buck, B.H., Langan, R., Eds.; Springer International Publishing: Cham, Switzerland, 2017; pp. 97–113.
11. Dekker, R. Applications of maintenance optimization models: A review and analysis. *Reliab. Eng. Syst. Saf.* **1996**, *51*, 229–240. [CrossRef]

12. Rinaldi, G.; Thies, P.R.; Johanning, L. Current Status and Future Trends in the Operation and Maintenance of Offshore Wind Turbines: A Review. *Energies* **2021**, *14*, 2484. [CrossRef]
13. Takata, S.; Kirnura, F.; van Houten, F.J.A.M.; Westkamper, E.; Shpitalni, M.; Ceglarek, D.; Lee, J. Maintenance: Changing Role in Life Cycle Management. *CIRP Ann.* **2004**, *53*, 643–655. [CrossRef]
14. Martin, R.; Lazakis, I.; Barbouchi, S.; Johanning, L. Sensitivity analysis of offshore wind farm operation and maintenance cost and availability. *Renew. Energy* **2016**, *85*, 1226–1236. [CrossRef]
15. Rinaldi, G.; Pillai, A.C.; Thies, P.R.; Johanning, L. Multi-objective optimization of the operation and maintenance assets of an offshore wind farm using genetic algorithms. *Wind Eng.* **2020**, *44*, 390–409. [CrossRef]
16. Rinaldi, G.; Thies, P.R.; Walker, R.; Johanning, L. A decision support model to optimise the operation and maintenance strategies of an offshore renewable energy farm. *Ocean Eng.* **2017**, *145*, 250–262. [CrossRef]
17. Dalgic, Y.; Lazakis, I.; Dinwoodie, I.; McMillan, D.; Revie, M. Advanced logistics planning for offshore wind farm operation and maintenance activities. *Ocean Eng.* **2015**, *101*, 211–226. [CrossRef]
18. Dinwoodie, I.; Endrerud, O.-E.V.; Hofmann, M.; Martin, R.; Sperstad, I.B. Reference Cases for Verification of Operation and Maintenance Simulation Models for Offshore Wind Farms. *Wind Eng.* **2015**, *39*, 1–14. [CrossRef]
19. Joschko, P.; Widok, A.H.; Appel, S.; Greiner, S.; Albers, H.; Page, B. Modeling and simulation of offshore wind farm O&M processes. *Environ. Impact Assess. Rev.* **2015**, *52*, 31–39.
20. Welte, T.M.; Sperstad, I.B.; Sørum, E.H.; Kolstad, M.L. Integration of Degradation Processes in a Strategic Offshore Wind Farm O&M Simulation Model. *Energies* **2017**, *10*, 925.
21. McMorland, J.; Collu, M.; McMillan, D.; Carroll, J. Operation and maintenance for floating wind turbines: A review. *Renew. Sustain. Energy Rev.* **2022**, *163*, 112499. [CrossRef]
22. Heijungs, R. On the number of Monte Carlo runs in comparative probabilistic LCA. *Int. J. Life Cycle Assess.* **2020**, *25*, 394–402. [CrossRef]
23. Pakenham, B.; Ermakova, A.; Mehmanparast, A. A Review of Life Extension Strategies for Offshore Wind Farms Using Techno-Economic Assessments. *Energies* **2021**, *14*, 1936. [CrossRef]
24. Pérez, B.; Mínguez, R.; Guanche, R. Offshore wind farm layout optimization using mathematical programming techniques. *Renew. Energy* **2013**, *53*, 389–399. [CrossRef]
25. Balasubramanian, K.; Thanikanti, S.B.; Subramaniam, U.; Sudhakar, N.; Sichilalu, S. A novel review on optimization techniques used in wind farm modelling. *Renew. Energy Focus* **2020**, *35*, 84–96. [CrossRef]
26. Ashuri, T.; Zaaijer, M.B.; Martins, J.R.R.A.; van Bussel, G.J.W.; van Kuik, G.A.M. Multidisciplinary design optimization of offshore wind turbines for minimum levelized cost of energy. *Renew. Energy* **2014**, *68*, 893–905. [CrossRef]
27. Yokoyama, R.; Shinano, Y.; Taniguchi, S.; Ohkura, M.; Wakui, T. Optimization of energy supply systems by MILP branch and bound method in consideration of hierarchical relationship between design and operation. *Energy Convers. Manag.* **2015**, *92*, 92–104. [CrossRef]
28. Buoro, D.; Casisi, M.; Pinamonti, P.; Reini, M. Optimal synthesis and operation of advanced energy supply systems for standard and domotic home. *Energy Convers. Manag.* **2012**, *60*, 96–105. [CrossRef]
29. Brodrick, P.G.; Brandt, A.R.; Durlofsky, L.J. Optimal design and operation of integrated solar combined cycles under emissions intensity constraints. *Appl. Energy* **2018**, *226*, 979–990. [CrossRef]
30. Mavrotas, G.; Diakoulaki, D.; Florios, K.; Georgiou, P. A mathematical programming framework for energy planning in services' sector buildings under uncertainty in load demand: The case of a hospital in Athens. *Energy Policy* **2008**, *36*, 2415–2429. [CrossRef]
31. Lozano, M.A.; Ramos, J.C.; Serra, L.M. Cost optimization of the design of CHCP (combined heat, cooling and power) systems under legal constraints. *Energy* **2010**, *35*, 794–805. [CrossRef]
32. Harb, H.; Reinhardt, J.; Streblow, R.; Müller, D. MIP approach for designing heating systems in residential buildings and neighbourhoods. *J. Build. Perform. Simul.* **2016**, *9*, 316–330. [CrossRef]
33. Samsatli, S.; Samsatli, N.J. A general spatio-temporal model of energy systems with a detailed account of transport and storage. *Comput. Chem. Eng.* **2015**, *80*, 155–176. [CrossRef]
34. Poncelet, K.; Delarue, E.; Duerinck, J.; Six, D.; D'haeseleer, W. *The Importance of Integrating the Variability of Renewables in Long-term Energy Planning Models*; KU Lueaven Energy Institute: Lueven, Belgium, 2014.
35. Mallapragada, D.S.; Papageorgiou, D.J.; Venkatesh, A.; Lara, C.L.; Grossmann, I.E. Impact of model resolution on scenario outcomes for electricity sector system expansion. *Energy* **2018**, *163*, 1231–1244. [CrossRef]
36. Oluleye, G.; Vasquez, L.; Smith, R.; Jobson, M. A multi-period Mixed Integer Linear Program for design of residential distributed energy centres with thermal demand data discretisation. *Sustain. Prod. Consum.* **2016**, *5*, 16–28. [CrossRef]
37. Menéndez, M.L.; Pardo, J.A.; Pardo, L.; Pardo, M.C. The Jensen-Shannon divergence. *J. Frankl. Inst.* **1997**, *334*, 307–318. [CrossRef]
38. National Climatic Center. *Typical Meteorological Year User's Manual TD-9734: Hourly Solar Radiation/Surface Meteorological Observations*; National Climatic Center, Ed.; National Climatic Center: Asheville, NC, USA, 1981.
39. Al-Mofeez, I.A.; Numan, M.Y.; Alshaibani, K.A.; Al-Maziad, F.A. Review of typical vs. synthesized energy modeling weather files. *J. Renew. Sustain. Energy* **2012**, *4*, 012702. [CrossRef]
40. Kullback, S.; Leibler, R.A. On Information and Sufficiency. *Ann. Math. Stat.* **1951**, *22*, 79–86. [CrossRef]
41. Huszár, F. How (not) to train your generative model: Scheduled sampling, likelihood, adversary? *arXiv* **2015**, arXiv:1511.05101.
42. Valamanesh, V.; Myers, A.T.; Arwade, S.R. Multivariate analysis of extreme metocean conditions for offshore wind turbines. *Struct. Saf.* **2015**, *55*, 60–69. [CrossRef]

43. Velarde, J.; Vanem, E.; Kramhøft, C.; Sørensen, J.D. Probabilistic analysis of offshore wind turbines under extreme resonant response: Application of environmental contour method. *Appl. Ocean. Res.* **2019**, *93*, 101947. [CrossRef]
44. Charlton, T.S.; Rouainia, M. Geotechnical fragility analysis of monopile foundations for offshore wind turbines in extreme storms. *Renew. Energy* **2022**, *182*, 1126–1140. [CrossRef]
45. Seyr, H.; Muskulus, M. Decision Support Models for Operations and Maintenance for Offshore Wind Farms: A Review. *Appl. Sci.* **2019**, *9*, 278. [CrossRef]
46. Dalgic, Y.; Lazakis, I.; Turan, O. Investigation of Optimum Crew Transfer Vessel Fleet for Offshore Wind Farm Maintenance Operations. *Wind Eng.* **2015**, *39*, 31–52. [CrossRef]
47. Kotzur, L.; Markewitz, P.; Robinius, M.; Stolten, D. Impact of different time series aggregation methods on optimal energy system design. *Renew. Energy* **2018**, *117*, 474–487. [CrossRef]
48. Poncelet, K.; Delarue, E.; Six, D.; Duerinck, J.; D'haeseleer, W. Impact of the level of temporal and operational detail in energy-system planning models. *Appl. Energy* **2016**, *162*, 631–643. [CrossRef]
49. Rinaldi, G. An Integrated Operation and Maintenance Framework for Offshore Renewable Energy. Ph.D. Thesis, University of Exeter, Exeter, UK, 2018.
50. Carroll, J.; McDonald, A.; McMillan, D. Failure rate, repair time and unscheduled O&M cost analysis of offshore wind turbines. *Wind Energy* **2016**, *19*, 1107–1119.
51. Warnock, J.; McMillan, D.; Pilgrim, J.A.; Shenton, S. Review of offshore cable reliability metrics. In Proceedings of the 13th IET International Conference on AC and DC Power Transmission (ACDC 2017), Manchester, UK, 14–16 February 2017; pp. 71–76.
52. Zhang, X.; Sun, L.; Sun, H.; Guo, Q.; Bai, X. Floating offshore wind turbine reliability analysis based on system grading and dynamic FTA. *J. Wind Eng. Ind. Aerodyn.* **2016**, *154*, 21–33. [CrossRef]
53. Kang, J.; Sun, L.; Guedes Soares, C. Fault Tree Analysis of floating offshore wind turbines. *Renew. Energy* **2019**, *133*, 1455–1467. [CrossRef]
54. Sperstad, I.B.; Stålhane, M.; Dinwoodie, I.; Endrerud, O.-E.V.; Martin, R.; Warner, E. Testing the robustness of optimal access vessel fleet selection for operation and maintenance of offshore wind farms. *Ocean Eng.* **2017**, *145*, 334–343. [CrossRef]
55. Bilbao, J.; Miguel, A.; Franco, J.; Ayuso, A. Test Reference Year Generation and Evaluation Methods in the Continental Mediterranean Area. *J. Appl. Meteorol.* **2004**, *43*, 390–400. [CrossRef]
56. Eames, M.; Ramallo-Gonzalez, A.; Wood, M. An update of the UK's test reference year: The implications of a revised climate on building design. *Build. Serv. Eng. Res. Technol.* **2016**, *37*, 316–333. [CrossRef]
57. Levermore, G.J.; Parkinson, J.B. Analyses and algorithms for new Test Reference Years and Design Summer Years for the UK. *Build. Serv. Eng. Res. Technol.* **2006**, *27*, 311–325. [CrossRef]
58. Pandit, R.K.; Kolios, A.; Infield, D. Data-driven weather forecasting models performance comparison for improving offshore wind turbine availability and maintenance. *IET Renew. Power Gener.* **2020**, *14*, 2386–2394. [CrossRef]
59. Xie, H.; Zhang, L.; Lim, C.P. Evolving CNN-LSTM Models for Time Series Prediction Using Enhanced Grey Wolf Optimizer. *IEEE Access* **2020**, *8*, 161519–161541. [CrossRef]
60. Xie, H.; Zhang, L.; Lim, C.P.; Yu, Y.; Liu, C.; Liu, H.; Walters, J. Improving K-means clustering with enhanced Firefly Algorithms. *Appl. Soft Comput.* **2019**, *84*, 105763. [CrossRef]
61. Xie, H.; Zhang, L.; Lim, C.P.; Yu, Y.; Liu, H. Feature Selection Using Enhanced Particle Swarm Optimisation for Classification Models. *Sensors* **2021**, *21*, 1816. [CrossRef]
62. Pillai, A.C.; Chick, J.; Khorasanchi, M.; Barbouchi, S.; Johanning, L. Application of an offshore wind farm layout optimization methodology at Middelgrunden wind farm. *Ocean Eng.* **2017**, *139*, 287–297. [CrossRef]
63. Pillai, A.C.; Thies, P.R.; Johanning, L. Mooring system design optimization using a surrogate assisted multi-objective genetic algorithm. *Eng. Optim.* **2019**, *51*, 1370–1392. [CrossRef]